Dynamical Climatology

Climatic effects of nuclear war: the role of atmospheric stability and ground heat fluxes.

by

J.F.B. Mitchell and A. Slingo

DCTN 58

August 1987

Meteorological Office (Met. O. 20)
London Road
Bracknell
Berkshire RG12 2SZ

DYNAMICAL CLIMATOLOGY TECHNICAL NOTE NO. 58

CLIMATIC EFFECTS OF NUCLEAR WAR: THE ROLE OF ATMOSPHERIC STABILITY AND GROUND HEAT FLUXES

by

J F B Mitchell and A Slingo

Submitted for publication in J. Geophys. Res.

Met O 20 (Dynamical
Climatology Branch)
Meteorological Office
London Road
Bracknell
Berkshire RG12 2SZ U.K.

August 1987

Note: This paper has not been published. Permission to quote from it should be obtained from the Assistant Director of the above Meteorological Office branch.

Climatic effects of nuclear war: the role of atmospheric stability and ground heat fluxes

J F B Mitchell and A Slingo[1]

Meteorological Office, Bracknell, Berks RG12 2SZ, UK

Abstract

Most studies of the climatic effects of nuclear war have used atmospheric models with simple representations of important physical processes. In this work, a model is used which treats the diurnal cycle of insolation, and includes surface and boundary layer parametrizations which take into account static stability and a four-layer soil model. Three idealized experiments are described in which a band of smoke is prescribed over northern mid-latitudes in July. In the first experiment, the standard model is used, in the second the effect of deep soil layers is ignored and in the third the stability dependence in the surface and boundary layer processes is removed. It is found that the inclusion of deep soil layers decreases the surface cooling by about 20%, whereas the inclusion of stability effects increases the cooling by about the same amount. Since these effects roughly cancel, previous studies which neglect them are probably not seriously in error in this regard.

---

1 On secondment to National Centre for Atmospheric Research, Boulder, Colorado.

1. Introduction

Most of the studies of the climatic effects of introducing large amounts of smoke and dust into the atmosphere (as has been speculated could happen following a nuclear war) have used atmospheric models with a rather crude treatment of the boundary layer and surface. The diurnal cycle of insolation may be omitted, the dependence of the surface fluxes of heat, moisture and momentum on static stability may be ignored, and no account is taken of the heat flux from deep soil layers (eg Covey et al, 1985; Malone et al, 1986). The simulation of surface temperature depends critically on the parametrisation of these processes. This note describes results from experiments carried out using a model which includes a full diurnal cycle, a treatment of the boundary layer and surface which takes into account atmospheric stability, and a four layer model of the soil. The model also has a somewhat higher horizontal resolution than used in other studies (eg Covey et al, 1985; Malone et al 1986; Ghan et al, 1987).

The objective of this study is to investigate the following problems -

1) How much would the inclusion of a heat flux from deep soil layers reduce the surface cooling?

2) On the other hand, how much would the use of a stability dependent boundary layer and surface exchange formulation reduce the downward heat flux due to the stable static stability expected in the lower atmosphere under the region of smoke and further increase the cooling of the land surface?

3) Would the inclusion of the diurnal cycle lead to increased vertical mixing near midday in the perturbation experiment, reducing the cooling found in the earlier studies?

4) Is the horizontal resolution used in earlier experiments inadequate to represent the transient disturbances which maintain the flow of maritime air over much of the mid-latitude continents in summer, when the baroclinicity of the atmosphere is weak? In summer, maritime air will tend to cool the land surface in the control simulation and warm the surface in the "nuclear winter" case, thus tending to reduce the difference between the unperturbed and perturbed cases.

It should be emphasized that this is a sensitivity study to examine the importance of the physical processes listed above. We have deliberately chosen the idealized smoke distribution of Covey et al (1984) to allow direct comparison with the results in that paper. For a more realistic simulation, the transport and removal of smoke should be included (eg Malone et al 1986).

2. Model and smoke parametrisation

The experiments reported were performed with the UK Meteorological Office 11-layer Atmospheric General Circulation Model. Simulations with a recent version were presented by Slingo and Pearson (1987). A detailed handbook is also available (Slingo 1985). Several improvements have since

been implemented, notably the inclusion of a parametrisation of orographic gravity-wave drag, revised formulations of penetrative convection and cloud prediction and a new land surface model. The latter employs four soil layers to represent more accurately the response of the surface temperature to diurnal and lower frequency forcing (Warrilow et al 1986). A paper describing the new model and its simulation is in preparation. Of particular importance to the present work is the inclusion of the land surface parametrisation and the fact that the model resolves the diurnal cycle (radiation and cloud schemes are called every three hours of model time) and includes stability-dependent calculations of the boundary-layer mixing and surface exchanges.

The effect of smoke was included by assuming that it absorbs, but does not scatter, solar radiation with an attenuation coefficient of 1.5 m^2 g-1. Surface fluxes and atmospheric heating rates from this simple treatment compare favourably with detailed multiple scattering calculations (Golding et al 1986). A similar approach was used by Covey et al (1984). To implement the parametrisation, existing code pertaining to the absorption by carbon dioxide was removed and the calculation of the transmission by smoke was substituted. In the standard version of the model, the absorption by water vapour, ozone and carbon dioxide are calculated separately and added to obtain the total gaseous absorption in a single spectral band. In the modified version, the total absorption is given by:

$$A_{TOT} = 1-T_{TOT} \qquad (1)$$

where the total transmission, T_{TOT}, is the product of that due to the combined effects of water vapour and ozone absorption, T_{WVO}, and that due to the smoke, T_{SMO}

$$T_{TOT} = T_{WVO} . T_{SMO} \quad (2)$$

The smoke transmission is:

$$T_{SMO} = \exp(-1.5u) \quad (3)$$

where u is the column density of smoke in g m-2 along the path. The absorption and emission of longwave radiation by the smoke is ignored for consistency with Covey et al, (1984).

3. The experiments

Three separate experiments were performed. In the first experiment (SMOKE), the modified version of the model as described in the previous section was used. In the second experiment (SOIL), the soil model was replaced by a single layer with a heat capacity equivalent to 5 cm water as in previous versions of the model. In the final experiment (STAB), the soil model was restored, but the boundary layer and surface exchange coefficients were set to those appropriate to neutral static stability. In each experiment, an anomaly integration was compared with a parallel control simulation in which no smoke was present.

In the anomaly integrations, 180 Teragrams of smoke were distributed evenly between 0 and 9 km and between 30 and 60°N on July 1. This gives a column absorption depth of 3 so that virtually no sunlight reaches the surface, and is similar to the perturbation considered by Covey et al (1984). We have restricted our attention to the northern hemisphere summer when the effects are likely to be largest. Each integration was run for 20 days using initial conditions for 1 July from a four year simulation with the standard model. The length of integration was chosen to be long enough to determine the maximum cooling, but short enough so that the assumption of a fixed distribution of smoke and prescribed sea surface temperatures is not unduly unrealistic.

4. Results

First we will describe the atmospheric response in experiment SMOKE and compare it to that obtained by Covey et al (1984) in a similar experiment using the NCAR Community Climate Model (CCM). Then we examine the sensitivity of the surface temperature changes to removing the deep soil layers and to removing the dependence of the boundary layer and surface fluxes on stability.

4.1 First experiment (SMOKE)

The absorption of solar radiation by the smoke rapidly warms the upper troposphere, by over 30K at 300 mb during the first 10 days and a further 25K during the second 10 days (Figure 1). There is no smoke and therefore no anomalous solar heating above 300 mb, but large scale

and convective motions adjust the temperature profile above the maximum warming towards the dry adiabat. Below 300 mb, the solar beam is gradually depleted and the warming decreases down to 600 mb, below which a cooling is observed. The solar flux is reduced to a few W/m2 at the surface and is much smaller than the net upward flux of longwave radiation. The surface cools rapidly during the first few days of the experiment (see later) and a strong inversion forms below 850 mb. Thus in the region of the smoke, the land surface no longer heats the atmosphere: instead a small amount of sensible heat is transferred downwards though the boundary layer to the surface. In a further experiment (described later) it was found that the magnitude of this flux is highly dependent on the formulation of vertical heat transfer in the lower atmosphere and at the surface.

The largest atmospheric warming and boundary layer cooling occur in the central latitude of the smoke band (Figure 2), but the upper level warming spreads both polewards and equatorwards so that, in the second 10 day period, the average warming near 20°S at 150 mb is almost 10K. The pattern of temperature changes is similar to Covey et al (1984) although the warming at upper levels is 10 to 20K less in SMOKE.

4.1.1 Changes in circulation

We now consider the resulting changes in circulation and how they contribute to the spread of the warming. As has been noted elsewhere (for example Cess, 1985) the large amount of absorbing smoke in the atmosphere reduces the albedo of the earth-

atmosphere system and produces the substantial increase in the depth averaged atmospheric temperature evident between 30 and 60°N in Figure 2. Above the middle troposphere, the warming raises the heights of constant pressure surfaces so that, for example, the height of the 200 mb surface increases by over 1200 m near 55N (Figure 3, upper curve). As might be expected from the geostrophic approximation, there is anomalous easterly flow at upper levels to the south of the maximum warming, and anomalous westerly flow to the north (Figure 4). The height anomaly is apparently too large to be maintained by purely geostrophic flow, and there is considerable down-gradient flow at upper levels leading to divergence above the smoke zone. The divergence of mass at upper levels produces a reduction in surface pressure in the smoke zone (Figure 3, lower curve). This produces anomalous low level westerly flow on the south side and easterly flow on the north side of the smoke zone, a reversal of the changes at upper levels (Figure 4). The divergence at upper levels must be balanced at lower levels by meridional convergence which would tend to confine the extent of the low level cooling. Of course, if smoke were advected with the atmospheric flow, the divergence at upper levels would increase the areal extent of the smoke cover and produce a more widespread cooling of the surface (Malone et al. 1986).

The geostrophic constraint is stronger in high latitudes (note that the gradient in the 200 mb field is greatest to the north of the anomaly), so the divergent flow at upper levels is

predominantly to the south of the height anomaly. The restricted area of the polar cap to the north of the anomaly may also limit the anomalous poleward mass flux. Indeed, the increased ascent in the smoke zone and the southward return flow at upper levels extend the main Hadley cell from 20°N (Figure 5a) to 40°N (Figure 5b). Note that in the perturbation experiment, there is strong southward flow at upper levels from the smoke zone into the southern hemisphere which is responsible for spread of the warming and enhanced easterly flow across the equator (Figures 2 and 4 respectively). The increase in 200 mb height immediately to the south of the equator is consistent with the height field adjusting to the easterly wind anomaly.

4.1.2 Surface temperature response

In the control simulation, the mean surface temperature over land between 30 and 60°N increases slowly through July (Figure 6) with an average daily range of about 15K. In SMOKE, the mean temperature falls by 11K in the first two days after the introduction of the smoke, mainly through longwave cooling to space. Thereafter, the cooling proceeds more slowly and reaches a maximum of about 25K at about 11 days, whereas the daily range of temperature is reduced to under 4K. The temperature then increases slightly, apparently because the increased westerly flow at low levels in the south of the smoke zone (Figure 4) strengthens the flow of warm maritime air across the cold continents.

The cooling is less rapid for the deeper soil layers (Figure 7). The top layer has a theoretical e-folding time of about 4 hours (see Warrilow et al. 1986) and thus reaches quasi-equilibrium with layer 2 very quickly. Layer 2 has an e-folding time of about 12 hours: layer 3, over 6 days and layer 4 about 85 days. The top 2 layers are in quasi-equilibrium with layer 3 after 2 to 3 days when all 3 layers cool at a similar rate. The progression of successively deep layers towards mutual equilibrium is similar to that described by Hasselmann (1979) for a diffusively coupled atmosphere, mixed-layer, deep ocean model. The deepest layer changes little during the course of the experiment due to its large thermal inertia. Note that the vertical temperature gradient is reversed during the first few days after the smoke is added, so that heat is transferred upwards, tending to delay and reduce the surface cooling. Of course, if the concentration of smoke were to be reduced and the experiment continued, the deep layers would then delay the subsequent warming of the surface.

The geographical distribution of the changes in surface temperature is far from uniform. Before the smoke was introduced, the temperature over land (30 to 60°N) generally exceeded 280K (Figure 8a). Two days after the introduction of the smoke (Figure 8b), the surface temperature falls below 270K in limited areas including the mountainous areas of North America and the Himalayas. After 10 days (Figure 8c), the temperature over most of North America, Europe and eastern Asia lying within

the smoke zone has fallen below 270K, and there are large areas where the temperature is less than 260K. On the other hand, along certain coasts such as the western United States and around inland seas, the temperature is considerably higher. Note that by day 20 there is a tendency for the cooling to be least over western regions of the continents (Figure 8d), consistent with the increase in onshore flow discussed above (see also Figure 4)

4.2 Experiment with a single soil layer (SOIL)

The above experiment was repeated, with a single soil layer in both the anomaly and control simulations. The depth of the soil was set at about twice that of the top layer in experiment SMOKE in order to produce a reasonable amplitude of the diurnal cycle of surface temperature. The surface cooled more rapidly than in SMOKE (Figure 9) reaching a minimum some 30K lower than in the control, 20% more than with the standard model treatment of the surface. The changes in atmospheric temperature are essentially the same as in SMOKE, except in the boundary layer where the cooling in the lowest 2 layers is respectively 3.8K and 1.4K greater than in SMOKE (Figure 10). This indicates that experiments ignoring deep soil layers exaggerate the surface cooling slightly, although this conclusion may be valid only for cases in which the surface is effectively decoupled from the free atmosphere, as here.

4.3 Neglect of stability dependence in the formulation of the bounday layer and surface exchanges. (STAB)

As noted in the introduction, many of the models used to date to study the effects of introducing large amounts of smoke and dust into the atmosphere neglect variations in static stability in calculating the vertical fluxes of heat, moisture and momentum at the surface and in the boundary layer. It has been noted that in cases of marked static stability (as found near the surface in Figure 1), this neglect would produce an unrealistically large down-gradient heat flux, and artificially warm the surface (eg Covey et al. 1984). The first experiment was therefore repeated, changing only the boundary layer and surface formulations, by prescribing coefficients appropriate to neutral stability in both anomaly and control simulations. Note that there is still a dependence on boundary layer height and wind shear in the determination of the vertical mixing coefficients in the boundary layer, and on the surface wind speed in the determination of the surface exchange coefficients. This change produced a substantial reduction in the surface cooling rate, and the maximum cooling was reduced by about 20% (Figure 9). The average downward flux of sensible heat was 31 Wm-2, averaged over days 11 to 20 in the anomaly experiment, as opposed to 7 and 10 Wm-2 in SMOKE and SOIL respectively. The surface inversion is much weaker than in the first two anomaly experiments, consistent with the higher surface temperature (Figure 10), but the layers above the inversion, particularly near 844 mb are colder than in the other two experiments. The changes at upper levels (not shown) are much the same.

5. Conclusions

It is perhaps fortuitous that the errors caused by the neglect of the effects of both the deeper soil layers and stability dependence are approximately equal and opposite. We therefore conclude that earlier experiments may not be greatly in error on this account, although one should bear in mind that these results are probably dependent on the parametrisations used, including the soil type and wetness. The major uncertainties in determining the climatic effects of a major nuclear conflict lie instead in the specification of the initial amount and distribution of smoke (see for example Penner, 1986) and in parametrizations of the removal by dry and wet deposition processes, which were not considered in this study.

6. Acknowledgements

We thank David Warrilow for advice on changing the surface layer formulation, and Roderick Smith for modifications to the boundary layer. Martin Cunnington ran the experiments and Kevin Needham was tireless in producing the necessary diagnostics.

7. References

Cess, R.D. 1985 Nuclear War: Illustrative effects of atmospheric smoke and dust upon solar radiation. Climatic Change 7, 237-251

Covey, C., Schneider, S.H., and Thompson, S.L. 1984 Global atmospheric effects of marine smoke injections from a nuclear war: Results from general circulation model simulations, Nature, 308, 21-25.

Covey, C., Thompson, S.L., and Schneider, S.H. 1985 A diagnosis of atmospheric general circulation model simulations. J. Geophys. Res. 90, 5615-5628.

Ghan, S.J., MacCracken, M.C. and Walton, J.J. 1987 The Climatic Response to large Atmospheric Smoke Injections: Sensitivity Studies with a Tropospheric General Circulation Model. Submitted to J.Geophys Res.

Golding, B.W., Goldsmith, P. Machin, N.A. and Slingo, A. 1986 The importance of local mesoscale factors in any assessment of the nuclear winter scenario. Nature, 319, 301-302

Hasselmann, K. 1979 "On the signal-to-noise problem in atmospheric response studies". In "Meteorology of the Tropical oceans", D.B. Shaw ed., Roy. Meteor. Soc., 251-259.

Malone, R.C., Auer, L.H., Glatzmaier, G.A., Wood, M.L. and Toon, O.B. 1986 Three-dimensional simulations including interactive transport, scavenging and solar heating of smoke. J. Geophys. Res. 91, 1039-1054

Penner, S.E. 1986 Uncertainties in the smoke source term for "nuclear winter" studies, Nature, 324, 222-226.

Slingo, A. (ed) 1985 Handbook of the Meteorological Office 11-layer atmospheric general circulation model. Volume 1: Model description DCTN 29. Meteorological Office (Met O 20), London Road, Bracknell, Berks RG12 2SZ.

Slingo, A. and Pearson, D.W. 1987 A comparison of the impact of an envelope orography and of a parametrization of orographic gravity-wave drag on model simulations. Quart. J.R. Met. Soc., 113, to appear in July issue.

Warrilow, D.A., Sangster, A.B. and Slingo, A. 1986 Modelling of land surface processes and their influence on European Climate DCTN 38. Meteorological Office (Met O 20), London Road, Bracknell, Berks RG12 2SZ.

Figure Captions

1. Vertical temperature profiles averaged over land between 30° and 60°N in experiment SMOKE. The horizontal lines represent pressure levels, the straight lines rising from left to right are isotherms, and rising from right to left are lines of constant potential temperature. The curved line is the 20°C moist adiabat.

   (a) Heavy solid lines; anomaly simulation averaged over days 1-10, 11-20 respectively.

   (b) Heavy dashed lines; as (a), but for the control simulation.

2. Height-latitude diagram of the changes in zonally-averaged temperature in experiment SMOKE, averaged over days 11-20. Contours every 10K with a dashed contour at 5K, areas of decrease stippled.

3. Zonally-averaged changes in experiment SMOKE, meaned over days 11-20.

   (a) Height of the 200 mb geopotential surface (dam)

   (b) Surface pressure (mb)

4. Height-latitude diagram of zonally-averaged changes in west to east wind component in experiment SMOKE, averaged over days 11-20. Contours every 10 ms^{-1}, areas of decrease stippled.

5. Stream function of mean meridional circulation (smoothed) averaged from day 11 to day 20 of experiment SMOKE.
Contours every 8 x 10^3 g s^{-1}, with dashed contours at + /- 4 x 10^3 g s^{-1}. Negative values (clockwise circulation) stippled.
(a) Control Simulation (b) Anomaly Simulation

6. Surface temperatures in experiment SMOKE averaged over land points between 30° and 60°N. Solid curve, daily maximum temperature; dashed curve, daily mean temperature; chain dotted curve, daily minimum temperature. Upper curves are from the control and lower curves from the anomaly experiment.

7. Changes in soil temperatures averaged over land between 30° and 60°N in experiment SMOKE. The curves are numbered in order of increasing depth and thickness.

8. Daily mean temperatures in experiment SMOKE. Contours every 10K, regions with temperature below 270K are stippled.

(a) July mean from the control simulation.
(b) Day 2 of the anomaly simulation.
(c) Day 10 of the anomaly simulation.
(d) Day 20 of the anomaly simulation.

9. Changes in daily mean surface temperature averaged over land between 30° and 60°N for the experiments with the three versions of the model.

10. Low level vertical temperature profiles, averaged over days 11-20. The grid is as in Figure 1 and the profiles from the control simulations are on the right. Solid lines, experiment SMOKE; dashed lines, experiment SOIL; chain dotted lines, experiment STAN.

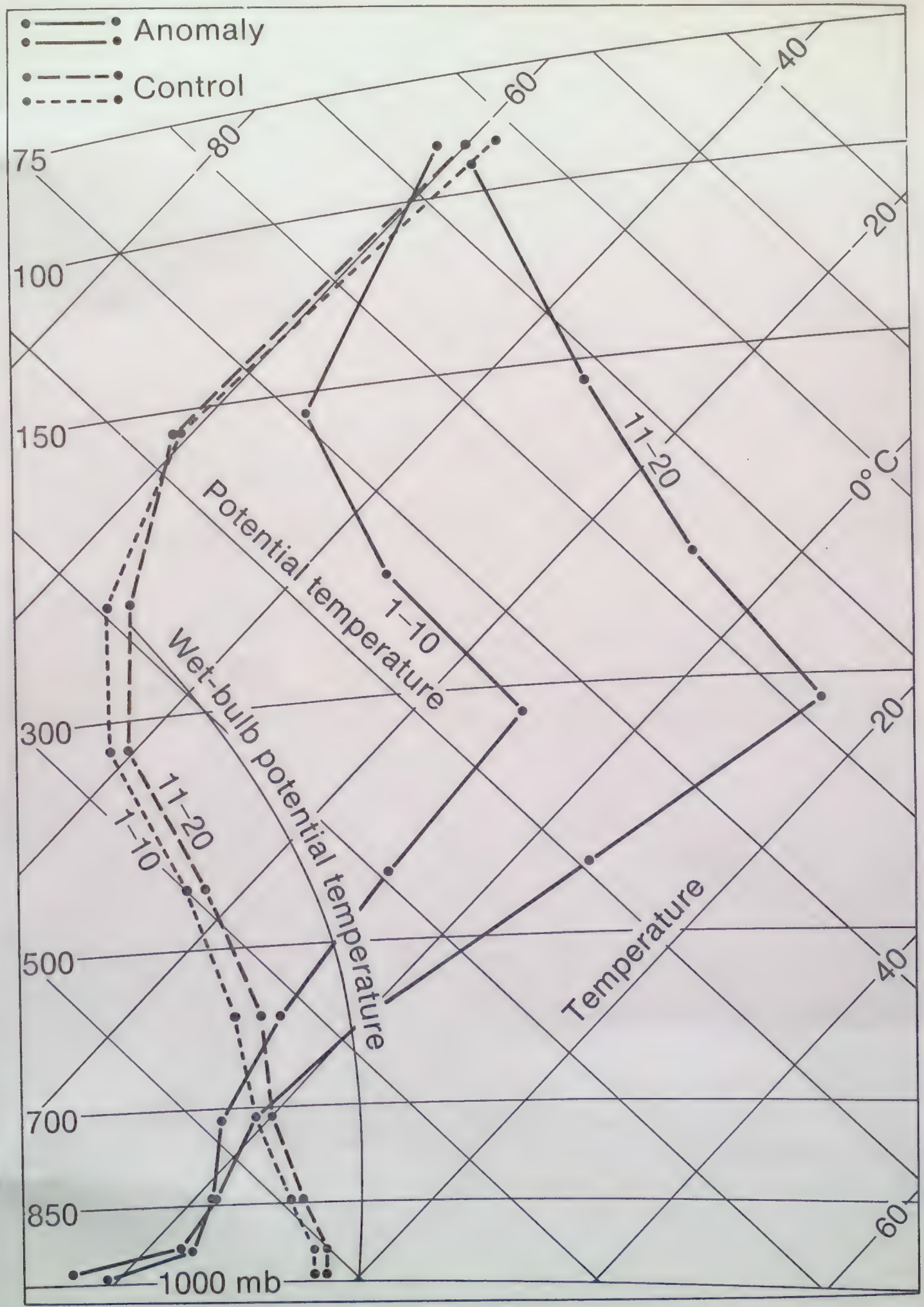
Anomaly
Control
75
100
150
300
500
700
850
1000 mb
80
60
40
20
0° C
20
40
60
Potential temperature
Wet-bulb potential temperature
Temperature
1–10
11–20
1–10
11–20

Figure 1

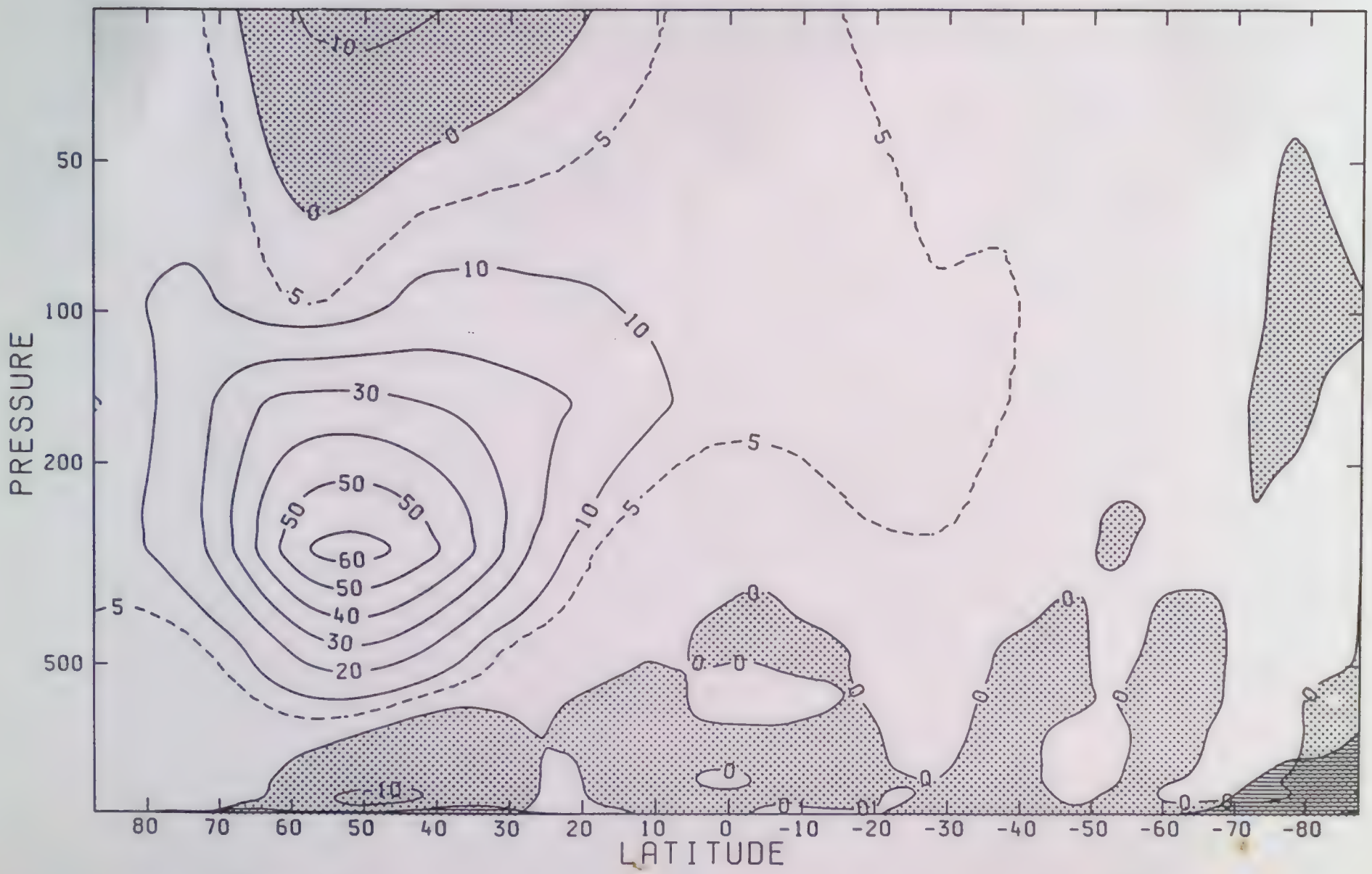
PRESSURE
50
100
200
500
80 70 60 50 40 30 20 10 0 -10 -20 -30 -40 -50 -60 -70 -80
LATITUDE
-10
0
5
10
30
50
60
40
20

Figure 2

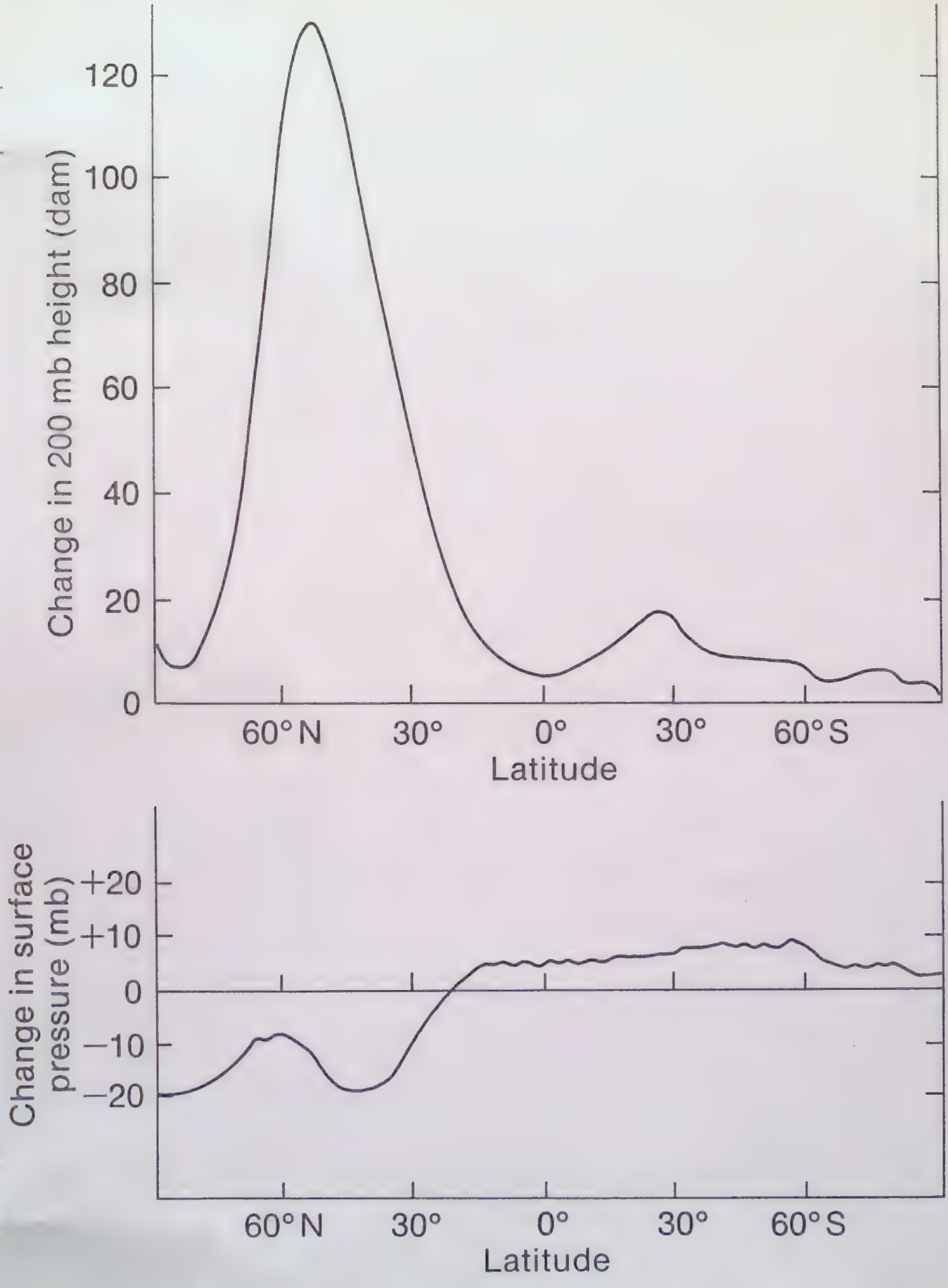
Change in 200 mb height (dam)
120
100
80
60
40
20
0
60° N
30°
0°
30°
60° S
Latitude
Change in surface pressure (mb)
+20
+10
0
−10
−20
60° N
30°
0°
30°
60° S
Latitude

Figure 3

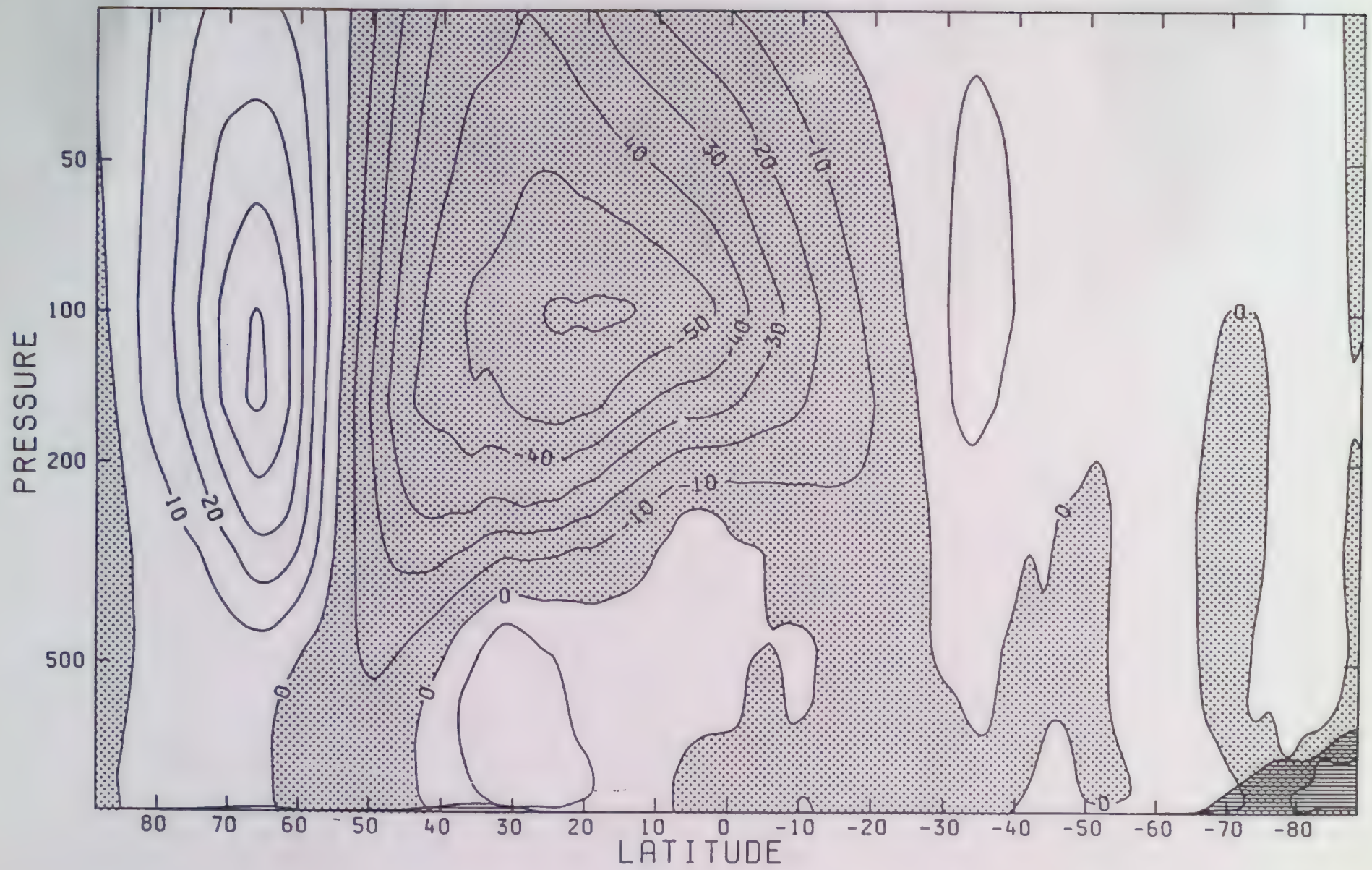
PRESSURE
50
100
200
500
LATITUDE
80
70
60
50
40
30
20
10
0
-10
-20
-30
-40
-50
-60
-70
-80
10
20
0
-10
-20
-30
-40
-50

Figure 4

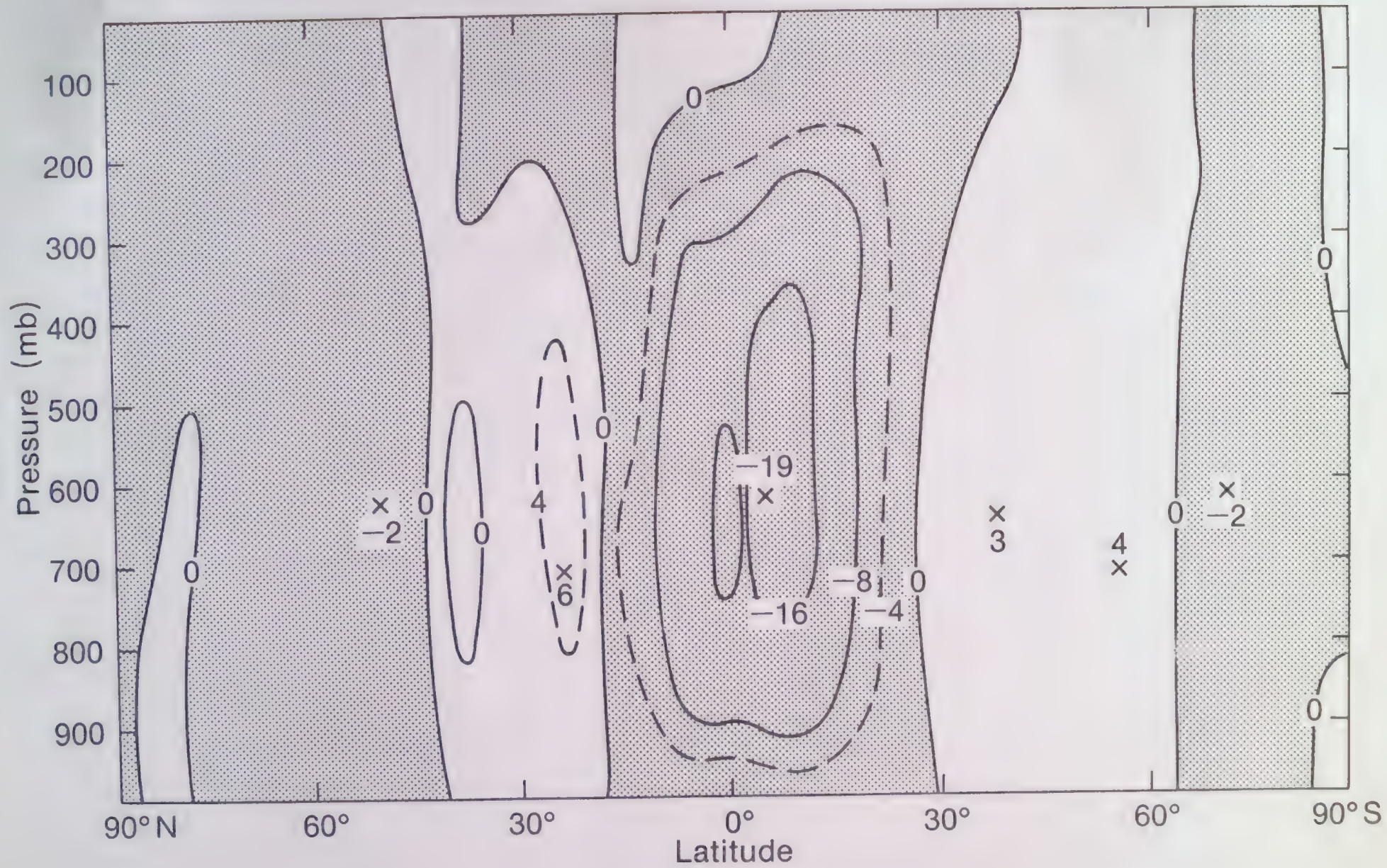

Pressure (mb)
100
200
300
400
500
600
700
800
900
90° N
60°
30°
0°
30°
60°
90° S
Latitude
0
−2
0
0
4
6
0
0
−19
−16
−8
−4
0
3
4
0
−2
0
0

Figure 5(a)

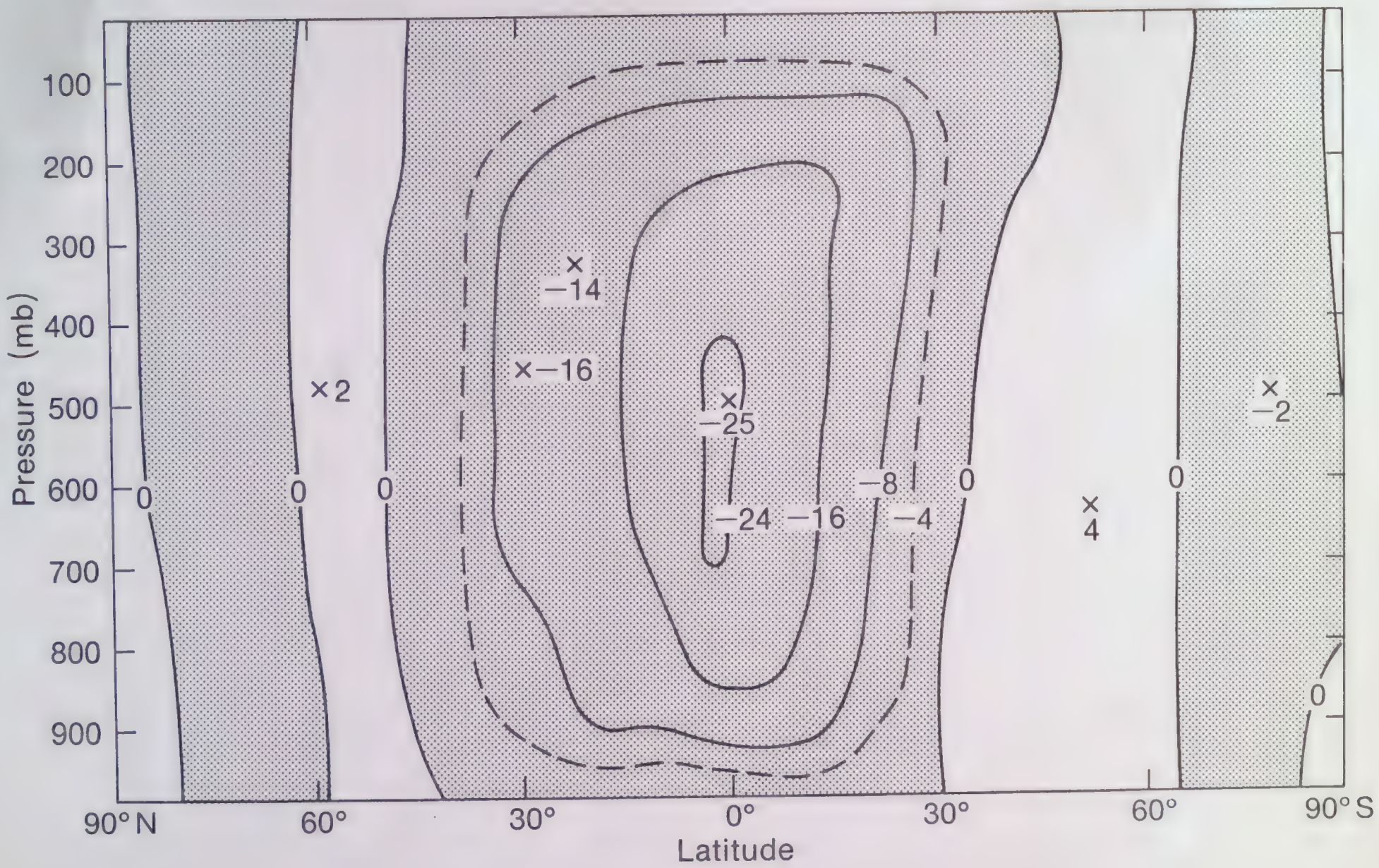
100
200
300
400
500
600
700
800
900
Pressure (mb)
×2
×−14
×−16
×−25
×4
×−2
0
0
0
−8
0
−24
−16
−4
0
0
90° N
60°
30°
0°
30°
60°
90° S
Latitude

Figure 5(b)

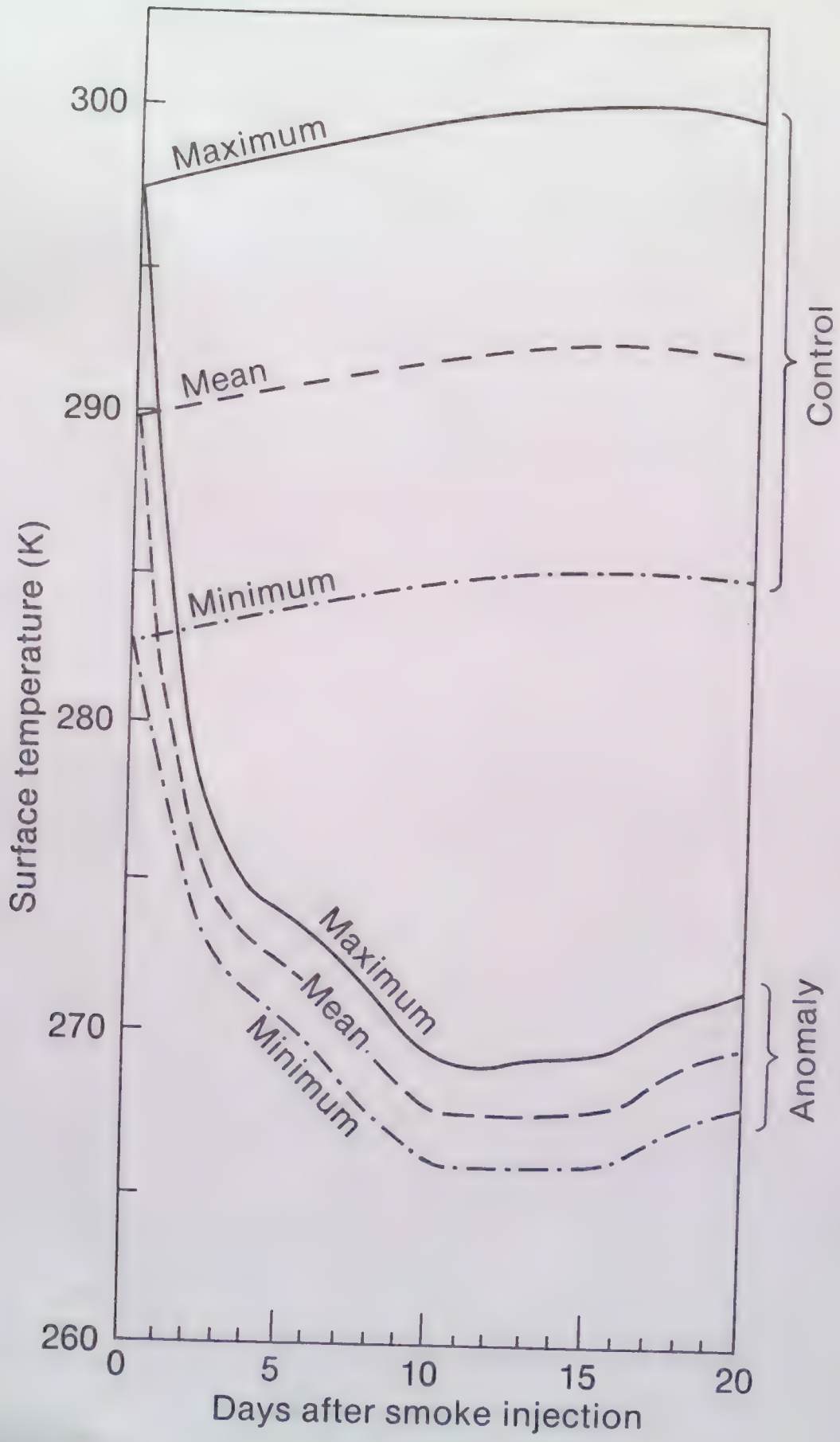
300
290
280
270
260
Surface temperature (K)
Maximum
Mean
Minimum
Control
Maximum
Mean
Minimum
Anomaly
0
5
10
15
20
Days after smoke injection

Figure 6

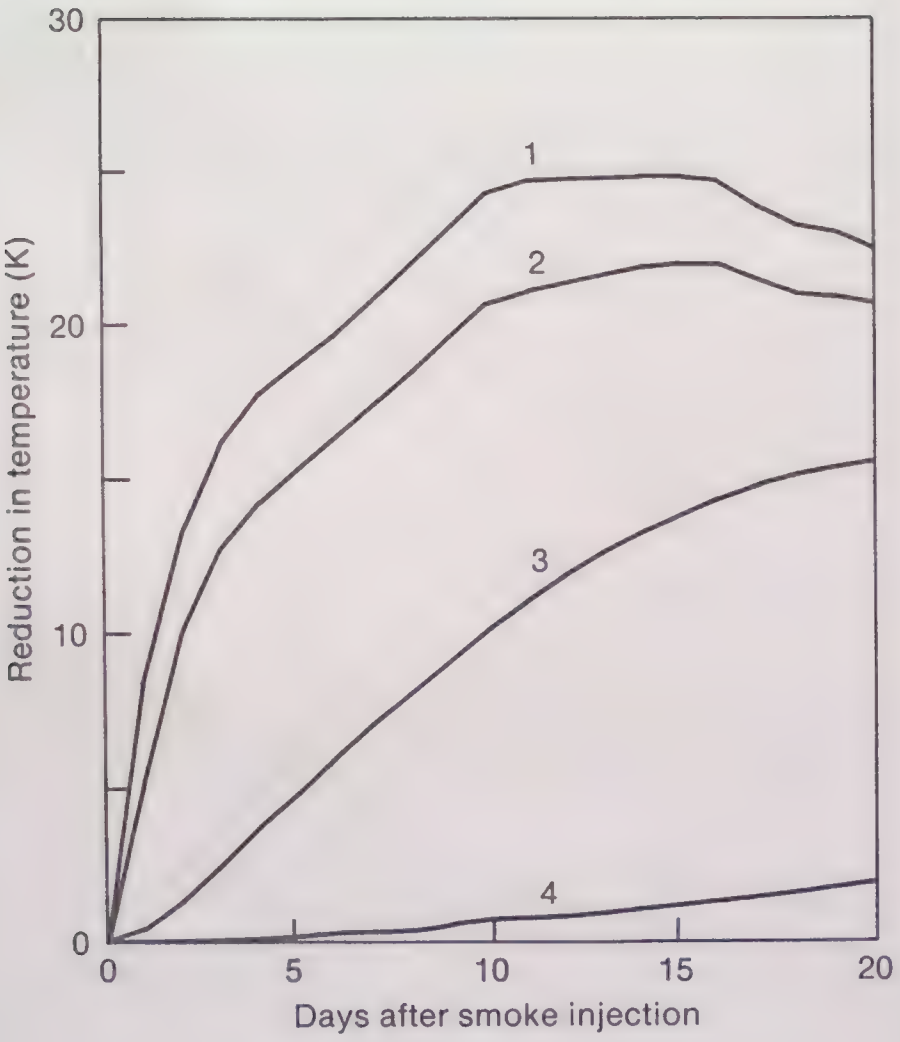
30
20
10
0
Reduction in temperature (K)
1
2
3
4
0
5
10
15
20
Days after smoke injection

Figure 7

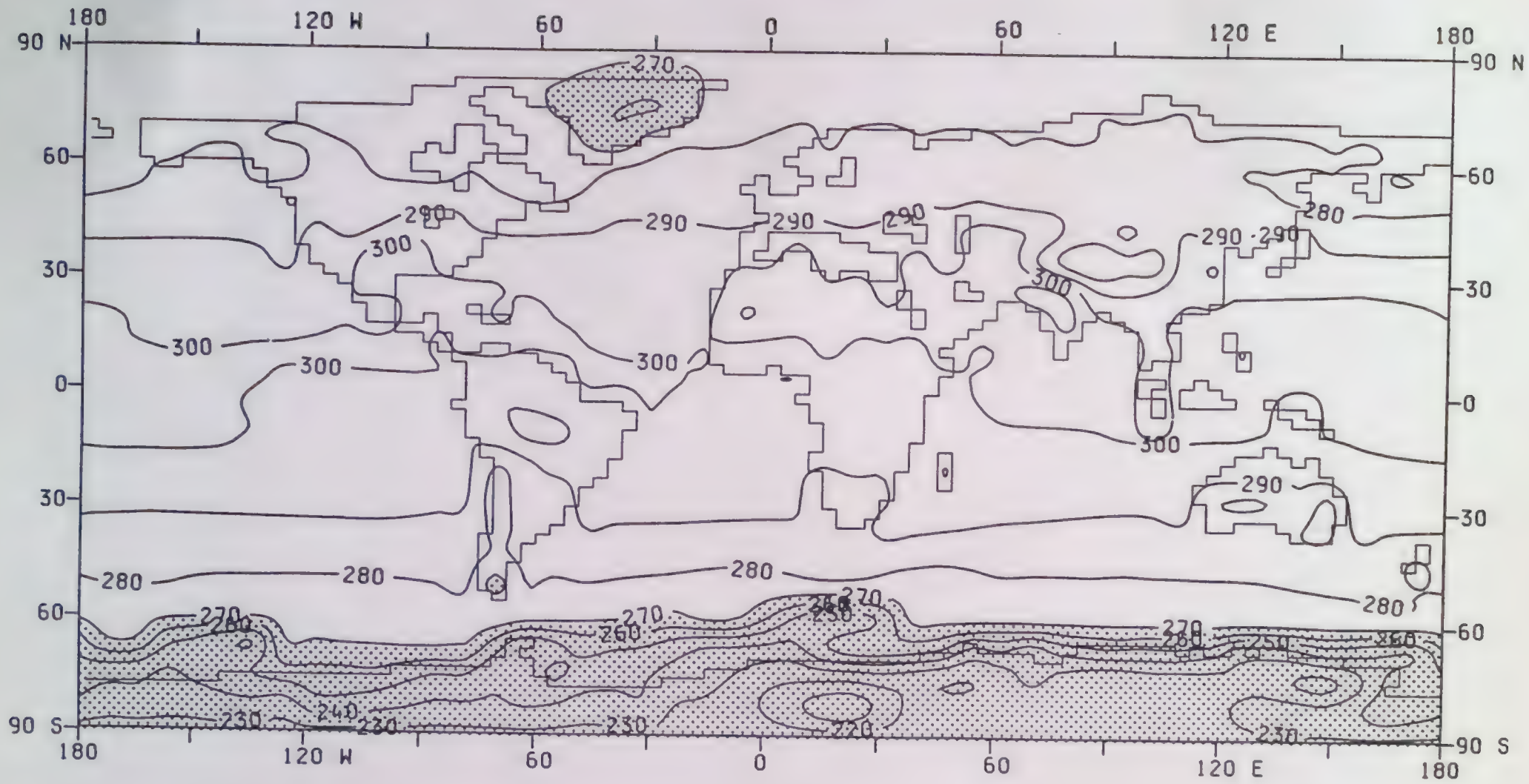
180
120 W
60
0
60
120 E
180
90 N
60
30
0
30
60
90 S
270
290
300
280
260
250
240
230

Figure 8a

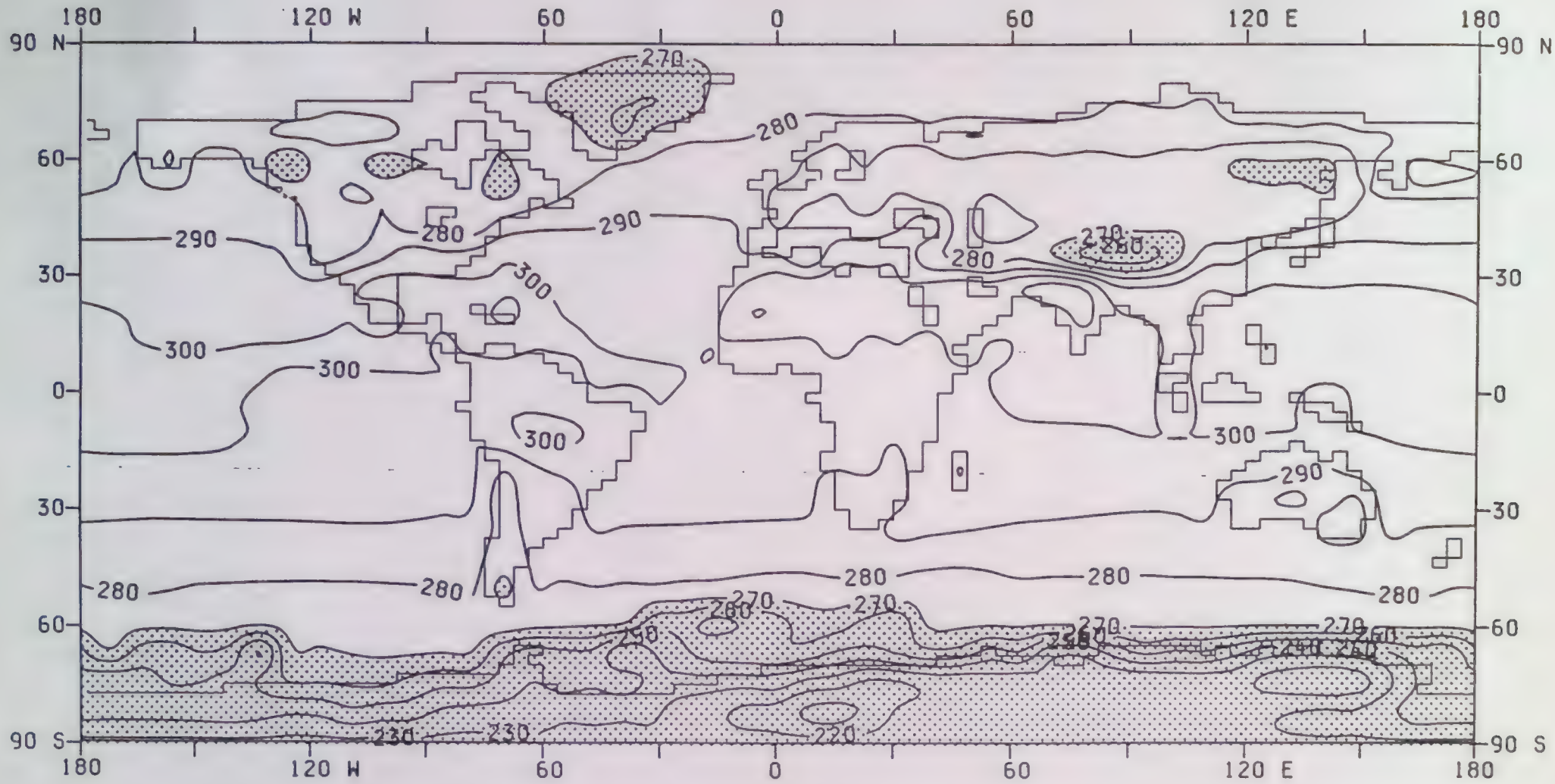
180
120 W
60
0
60
120 E
180
90 N
60
30
0
30
60
90 S
270
280
290
300
230
220

Figure 8b

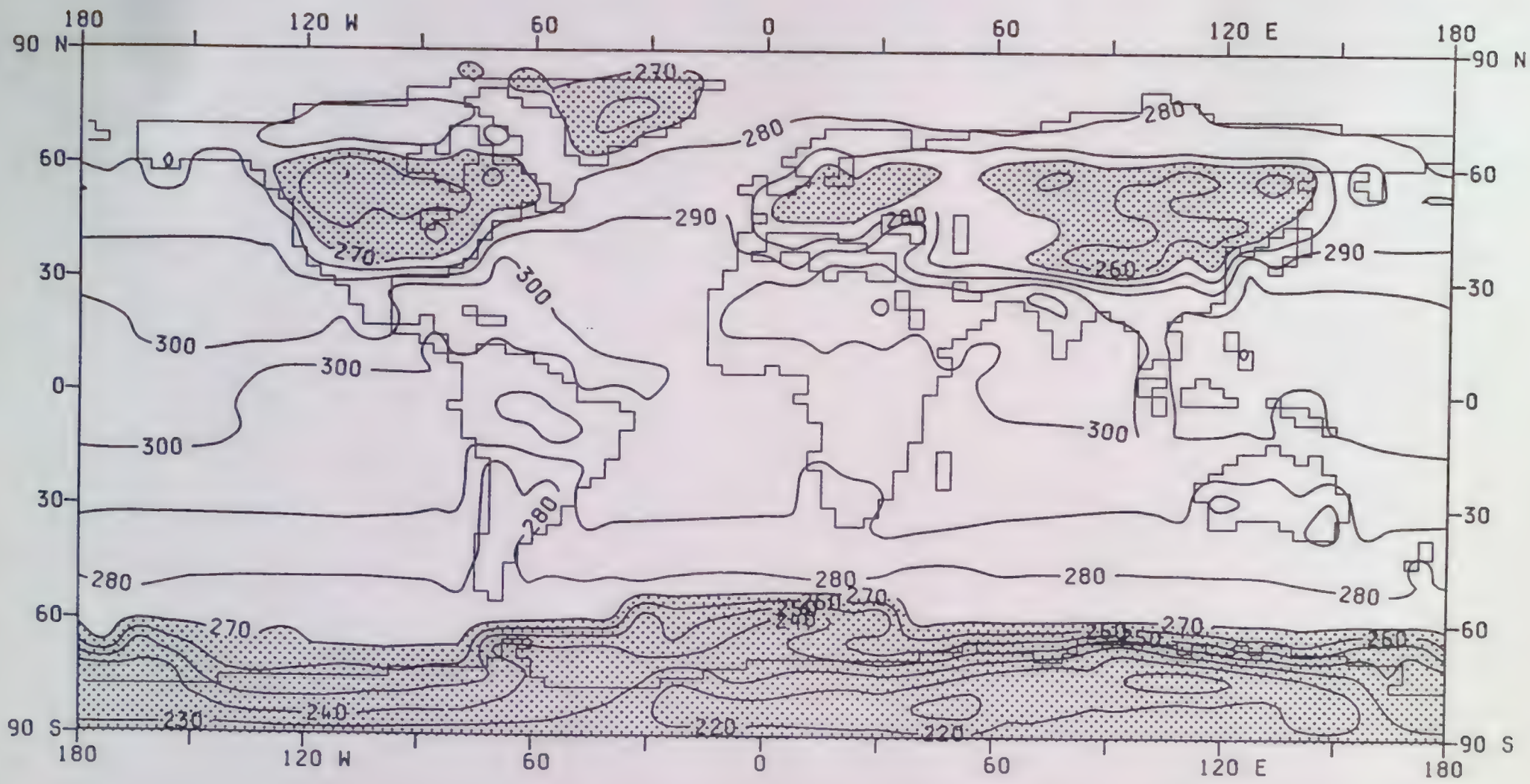
180
120 W
60
0
60
120 E
180
90 N
60
30
0
30
60
90 S
270
280
290
300
260
240
230
220

Figure 8c

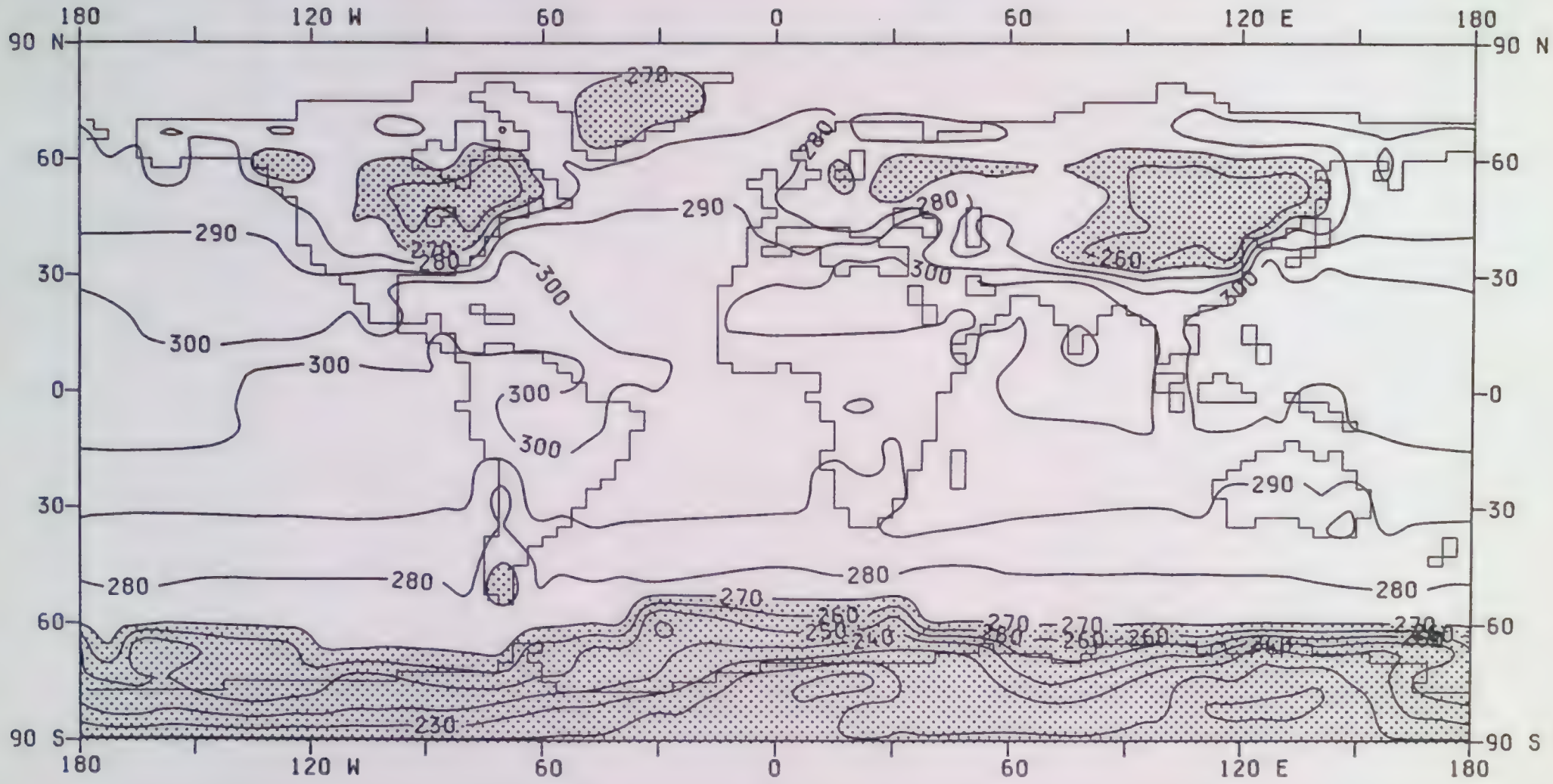
180
120 W
60
0
60
120 E
180
90 N
60
30
0
30
60
90 S
270
280
290
300
260
240
230

Figure 8d

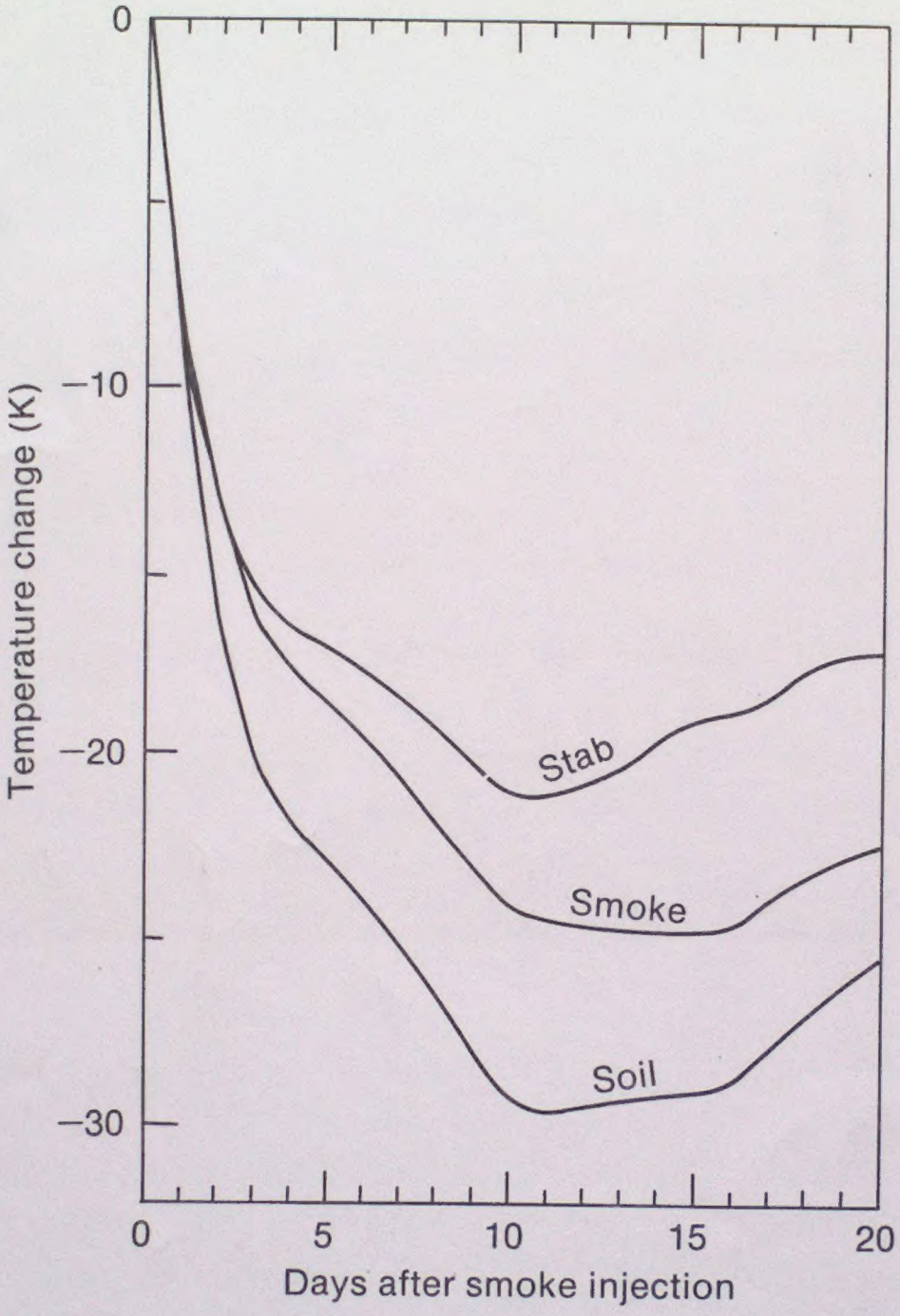
0
−10
−20
−30
Temperature change (K)
Stab
Smoke
Soil
0
5
10
15
20
Days after smoke injection

Figure 9

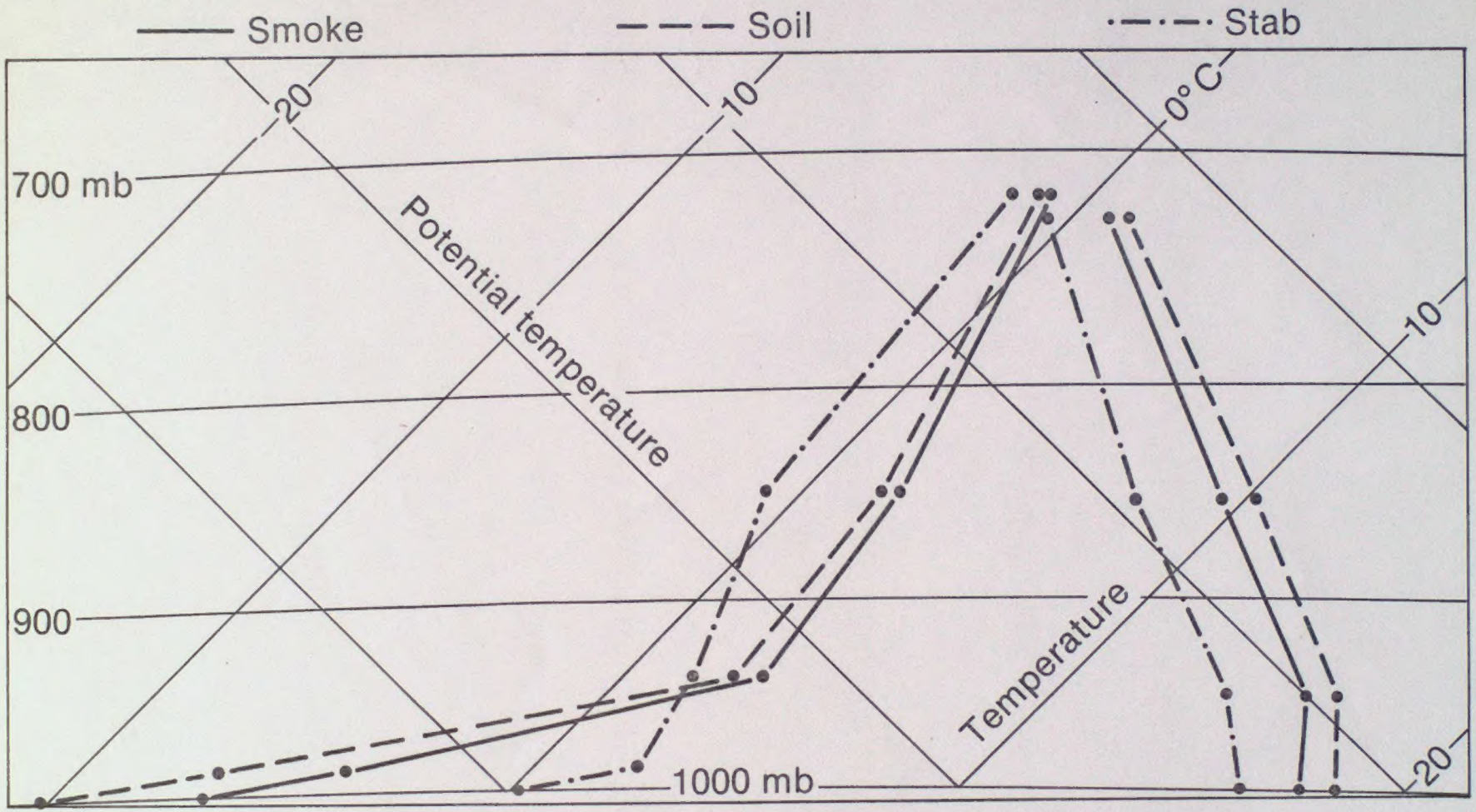
Smoke
Soil
Stab
20
10
0° C
700 mb
Potential temperature
800
10
900
Temperature
1000 mb
20

Figure 10

DYNAMICAL CLIMATOLOGY TECHNICAL NOTES

DCTN 1 June 1984
A scheme for incorporating the thermodynamic sea-ice model into a coupled ocean-atmosphere model.
C Gordon and M Bottomley

DCTN 2 Sept 1984
The parametrization of the upper ocean mixed layer in coupled ocean/atmosphere models.
C Gordon and M Bottomley

DCTN 3 Sept 1984
The response of a simple thermodynamic sea-ice model to GCM forcing appropriate for perennial sea-ice.
M Bottomley

DCTN 4 Sept 1984
Potential vorticity in the stratosphere derived using data from satellites.
S A Clough, M S Grahame and A O'Neill

DCTN 5 Sept 1984
Simulation of the seasonal cycle of SST using globally specified climatological data to force simple ocean models.
M S Grahame

DCTN 6 Sept 1984
Development of an improved GCM radiation scheme.
A Slingo and R C Wilderspin

DCTN 7 Sept 1984
On the specification of surface fluxes in coupled atmosphere/ocean general circulation models.
J F B Mitchell, C A Wilson and C M Price

DCTN 8 Sept 1984
A survey of possible repercussions of the Soviet river reversal programme on Arctic sea-ice.
H Cattle

DCTN 9 Oct 1984
A study of a strong stratospheric warming during January 1982
T D A Fairlie

DCTN 10 Nov 1984
An intercomparison of the Met O 11 M45 model and the Met O 20 11-level model on the Cyber 205
J F Dyson

DCTN 11 Nov 1984
Simulation of observed time series of temperature and precipitation over eastern England.
D M Reed

DCTN 12 Nov 1984
Forecasts and analyses of the onset of the Southwest monsoon.
R Kershaw

DCTN 13 Nov 1984
On modelling the effects of CO_2 on climate.
J F B Mitchell

DCTN 14 Dec 1984
Development of a revised longwave radiation scheme for an atmospheric general circulation model.
A Slingo and R C Wilderspin

DCTN 15 Jan 1985
Rossby wavetrains in the stratosphere forced by localised disturbances in the troposphere.
C J Marks (Oxford), A O'Neill and V D Pope

DYNAMICAL CLIMATOLOGY TECHNICAL NOTES

DCTN 16 Jan 1985
Observing system experiments using the Meteorological Office's 15-level model.
M A Bromley

DCTN 17 Feb 1985
Atmospheric general circulation simulation of the climate of the Mediterranean region.
H Cattle

DCTN 18 Feb 1985
Diurnal variation and cloud in a general circulation model.
C A Wilson and J F B Mitchell

DCTN 19 Feb 1985
The sensitivity of the Saharan region in a general circulation model.
W M Cunnington and P R Rowntree

DCTN 20 Mar 1985
The impact of aircraft observations on analyses and forecasts from the operational 15-level model.
B H Barwell

DCTN 21 Mar 1985
Non-linear effects on heat-induced circulation of the tropical atmosphere.
A E Gill and P J Phlips

DCTN 22 Apr 1985
Simulation of cloudiness with the U.K. Meteorological Office 11-layer AGCM.
A Slingo and R C Wilderspin

DCTN 23 Apr 1985
An integrated approach to the representation of cloud processes. R N B Smith

DCTN 24 May 1985
Nuclear Winter: Calculations of the shortwave radiative effects of soot aerosols.
A Slingo and P Goldsmith

DCTN 25 Jul 1985
Sea ice and the Antarctic winter circulation: a numerical experiment.
J F B Mitchell and T S Hills

DCTN 26 Jul 1985
A Budyko-Sellers model for study of ocean-atmosphere interaction.
W J Ingram

DCTN 27 Aug 1985
The effect of a shoaling thermocline on equatorially-trapped Kelvin waves.
A E Gill and B A King

DCTN 28 Sept 1985
CO_2 climate sensitivity and model dependence of results.
J F B Mitchell, C A Wilson and W M Cunnington

DCTN 29 Sept 1985
Handbook of the Meteorological Office 11-layer atmospheric general circulation model.
Volume 1 : Model Description
Edited by A Slingo

DCTN 30 Sept 1985
Impact of land surface variations on African rainfall in general circulation models.
P R Rowntree, M F Wilson and A B Sangster

DCTN 31 Nov 1985 The annual cycle of sea level in the eastern tropical Pacific.
G R Bigg and A E Gill

DCTN 32 Nov 1985 An analytic model of the heat-induced tropical circulation in the presence of a mean wind.
P J Phlips and A E Gill

DCTN 33 Nov 1985 The effect of resolution and diffusion on the simulated climate.
J F Dyson

DCTN 34 Jan 1986 Rossby adjustment over a step.
M K Davey, A E Gill, E R Johnson and P F Linden

DCTN 35 Jan 1986 Issues concerning the evaluation of effective surface roughness of heterogeneous terrain.
D J Carson

DCTN 36 Mar 1986 Climate sensitivity and past climates : evidence from numerical studies
J F B Mitchell

DCTN 37 Mar 1986 Parametrizations of land-surface processes in Meteorological Office numerical weather prediction and climate models
D J Carson

DCTN 38 Apr 1986 Modelling of land-surface processes and their influence on European Climate
D A Warrilow, A B Sangster and A Slingo

DCTN 39 Apr 1986 Simulation of climatic change due to increased CO_2
J F B Mitchell

DCTN 40 May 1986 On the interpretation of the Eliassen-Palm flux divergence.
Part I : Theory
D G Andrews

DCTN 41 June 1986 Experiments on tropical circulation with a simple moist model.
M K Davey and A E Gill

DCTN 42 Jun 1986 Parameter regimes for studying isolated eddies.
P D Killworth and M K Davey

DCTN 43 Jun 1986 A comparison of the impact of an envelope orography and of a parametrization of orographic gravity-wave drag on model simulations.
A Slingo and D W Pearson

DCTN 44 Jul 1986 The effect of a sea-surface temperature anomaly on a prediction of the onset of the south-west monsoon over India.
R Kershaw

DCTN 45 Jul 1986 An introduction to the parametrization of land-surface processes.
D J Carson

DYNAMICAL CLIMATOLOGY TECHNICAL NOTES

DCTN 46 Sept 1986 Lateral boundaries and the heat-induced flow in the tropical atmosphere.
P J Phlips and A E Gill

DCTN 47 Nov 1986 Simulation of the diurnal cycle of outgoing longwave radiation with an atmospheric GCM.
A Slingo, R C Wilderspin and S J Brentnall

DCTN 48 Feb 1987 A 2 x CO_2 climate sensitivity experiment with a global climate model including a simple ocean
C A Wilson and J F B Mitchell

DCTN 49 Feb 1987 Sensitivity of the Met O 20 11-layer model to increased land surface roughness length
C C Heasman

DCTN 50 Feb 1987 The influence of atmospheric waves on the general circulation of the middle atmosphere
D G Andrews

DCTN 51 Feb 1987 Transport mechanisms in the middle atmosphere: an introductory survey
D G Andrews

DCTN 52 Mar 1987 The Met O 20 stratosphere-mesosphere model
M Pisher

DCTN 53 Apr 1987 Simulations of linear and nonlinear disturbances in the stratosphere
A O'Neill and V D Pope

DCTN 54 Apr 1987 Aspects of dynamics of the middle atmosphere inferred using data from a satellite and from a numerical model
T D A Fairlie and A O'Neill

DCTN 55 Apr 1987 The seasonal evolution of the stratosphere in the northern hemisphere
A O'Neill and V D Pope

DCTN 56 Apr 1987 The adjustment of mumerical weather prediction models to local perturbations
B R Barwell and R A Bromley

DCTN 57 Jun 1987 Climate simulations for 9000 years before present: Seasonal variations and the effect of the Laurentide ice sheet
J F B Mitchell, N S Grahame and K J Needham